Cretaceous Research (2001) **22**, 481–490
doi:10.1006/cres.2001.0271, available online at http://www.idealibrary.com on IDEAL®

The Cenomanian–Turonian anoxic event in southern Tibet

***C. S. Wang, *X. M. Hu, †L. Jansa, ‡X. Q. Wan and *R. Tao**

**Chengdu University of Technology, 610059, Chengdu, China; e-mail: wcs@cdut.edu.cn*
†*Earth Science Department, Dalhousie University, Halifax, NS, Canada*
‡*Department of Geosciences, China University of Geosciences, 100083, Beijing, China*

Revised manuscript accepted 31 May 2001

The Cenomanian–Turonian black shales in southern Tibet record a global oceanic anoxic event (OAE). A combined sedimentological, geochemical and micropalaeontological study shows: (1) increased total organic carbon (TOC: 0.5–1.7%) with a peak accumulation across the Cenomanian/Turonian boundary (CTB); (2) sulfur/carbon ratios (S/C) and high degree of pyritization (DOP) indicating that the depositional environment in the Gyangze area was oxygen-depleted and H_2S-rich, while synchronous, shallower deposits in the Gamba area accumulated in an oxic environment; (3) bulk-rock $\delta^{13}C$ analyses of carbonates indicating a positive 2‰ excursion across the CTB, similar to that observed in the western Tethys and Pacific; and (4) an extinction rate of planktic foraminifera across the CTB reaching 50–70%, while the extinction of benthic foraminifera was as high as 90%. A major extinction of benthic foraminifera indicates the development of an inhospitable environment associated with the presence of poorly oxygenated bottom waters. The CTB OAE in Tibet documents a fundamental change in Late Cretaceous palaeoceanography associated with increased dispersal of the southern continents. As the Indian plate moved northward, there was a change in ocean circulation which may have led to the development of a layer of poorly oxygenated bottom and intermediate waters within both the western and eastern Tethys.

KEY WORDS: oceanic anoxic events; Cenomanian/Turonian boundary; southern Tibet.

1. Introduction

Organic-rich black shales are widespread within Berriasian–Turonian marine sedimentary deposits of the Tethys. Their occurrence has been mostly explained by deposition in a poorly oxygenated environment. Several of these organic-rich intervals have an ocean-wide distribution and are known as 'Oceanic Anoxic Events' (OAEs) associated with positive $\delta^{13}C$ anomalies (Schlanger & Jenkyns, 1976; Jenkyns, 1980). One anomaly occurs at the Cenomanian/Turonian boundary (CTB OAE2). This has been recorded in widespread locations (Bralower, 1988), including southern Germany (Hilbrecht & Dahmer, 1994), southern England (Jarvis *et al.*, 1988; Leary *et al.*, 1989), southern France (Crumière, 1988), southeastern Poland (Peryt & Wyrwicka, 1991), northern Spain (Paul *et al.*, 1994), northern Japan (Hasegawa & Saito, 1993), India (Govindan & Ramesh, 1995), the Atlantic Ocean Basin (Herbin *et al.*, 1987, ODP Leg 103), and Brazil (Mello *et al.*, 1989). The CTB OAE developed in deep ocean basins, on continental slopes, on submarine plateaux and in epicontinental seas (Schlanger *et al.*, 1987; Reyment & Bengtson, 1986). However, the circumstances causing this event remain a matter of speculation. The objective of this paper is to describe the occurrence of black shales of Cenomanian/Turonian-boundary age in southern Tibet, and to consider the palaeoceanographic implications of this occurrence and their potential significance as source rocks for hydrocarbon generation in southern Tibet.

2. Geologic setting and biostratigraphy

The study area is located to the south of the Yarlung Zangbo Suture Zone in the Tethyan Himalayas. During the mid Cretaceous this region was located at a latitude of *c.* 21°S (Patzelt *et al.*, 1996), and was surrounded by an ocean connected eastward to the Pacific Ocean and westward to the Mediterranean Tethys. Two Cretaceous localities near the towns of Gamba and Gyangze were studied in detail. Although both localities are not far apart, they represent different depositional settings on a northern passive continental margin of the Indian plate (Yu & Wang, 1990) (Figure 1). East of Gamba, at Zongshan

0195–6671/01/040481+10 $35.00/0

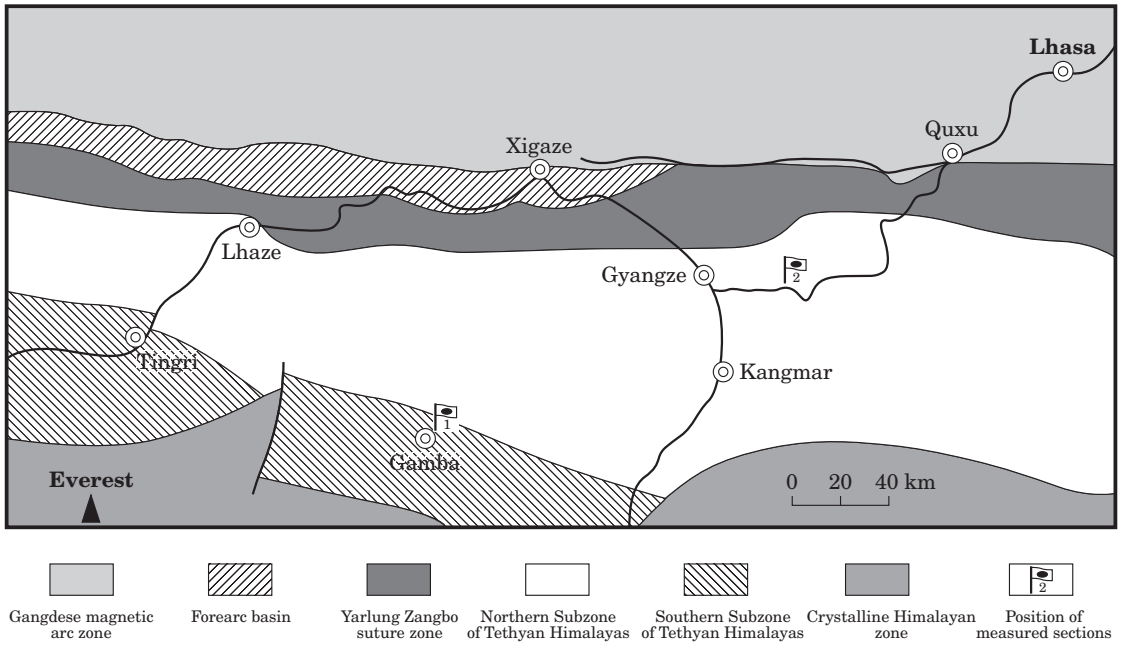

Figure 1. Generalized geological map of the central part of southern Tibet, showing the localities studied: 1, Zongshan east of Gamba; 2, Gyabula, east of Gyangze.

(Figure 1), the Cretaceous sedimentary deposits consist predominantly of intercalated glauconite-bearing, fine-grained quartzose and calcareous sandstones, fossiliferous mudstones and hemipelagic limestones. The succession has been subdivided into the Dongshan, Chaqiela, Lengqingre, Xiawuchubo, Jiubao and Zongshan formations (Wan, 1985; Xu *et al.*, 1990), which have been described in detail by Mu *et al.* (1973), Wen (1974), Wan (1985), Xu *et al.* (1990), Willems & Zhang (1993) and Liu & Einsele (1994) (Figure 2). They are considered to reflect deposition on a deepening shelf to upper slope, as discussed in more detail below.

A study of the microfauna of the Gamba succession shows that the top of the late Cenomanian *Rotalipora cushmani* Zone is marked by the last occurrence of the planktic foraminifera *Rotalipora greenhornensis* and *Hedbergella trocoidea,* and of the benthic foraminifera *Lenticulina franki, Gyroidina excerta* and *Gyroidinides primitiva* (Figure 3; for authors of all taxa noted in this paper, see Appendix). The *Whiteinella archaeocretacea* Zone extends from the last occurrence of *Rotalipora cushmani* at the base to the first occurrence of *Helvetoglobotruncana helvetica* at the top (Figure 3). The first occurrence of *H. helvetica* is regarded as the base of the early Turonian *Helvetoglobotruncana helvetica* Zone (Figure 3). All three foraminiferal zones are present within the upper Lengqingre and lower Xiawuchubo formations (Figure 2). The *W. archaeocretacea* Zone corresponds to the strata from 90.6 to 125.2 m (Figure 3). A significant change in the foraminiferal assemblage occurs in the *W. archaeocretacea* Zone. The diversity and abundance of the components of the assemblage decrease continuously from 93.7 m upwards through the section until foraminifera are no longer present at 102.2 m. They reappear at 103.2 m (Figure 3), and the first occurrence of *Helvetoglobotruncana praehelvetica* is immediately above this level. There was an obvious extinction bioevent during this depositional interval at 102.2–103.2 m (see below for details). The CTB at Zongshan, as defined by the first occurrence of *Helvetoglobotruncana praehelvetica,* has been placed at 103.2 m within the *Whiteinella archaeocretacea* Zone (Wan *et al.*, 1997).

In the Gyangze area, the Cretaceous strata consist mainly of black shales. Recently, Li *et al.* (1999) and Wang *et al.* (2000) redefined the Mesozoic strata in the Gyangze area and subdivided the Cretaceous succession into the Gyabula, Chuangde, and Zongzhuo formations (Figure 2), with boundaries that are markedly different from those recognised by previous authors (e.g., Wen, 1974; Wu, 1987). The Gyabula Formation is composed of black shales with frequent pyrite nodules, intercalated with turbiditic sandstones. A Berriasian–Santonian age for the formation is supported by the occurrence of various radiolarians including *Eucyriticium* sp., *Hemicryptocapsa* sp., *Pseudoaulacophacus floresensis*, and *Theocampe tina*. The overlying Chuangde Formation

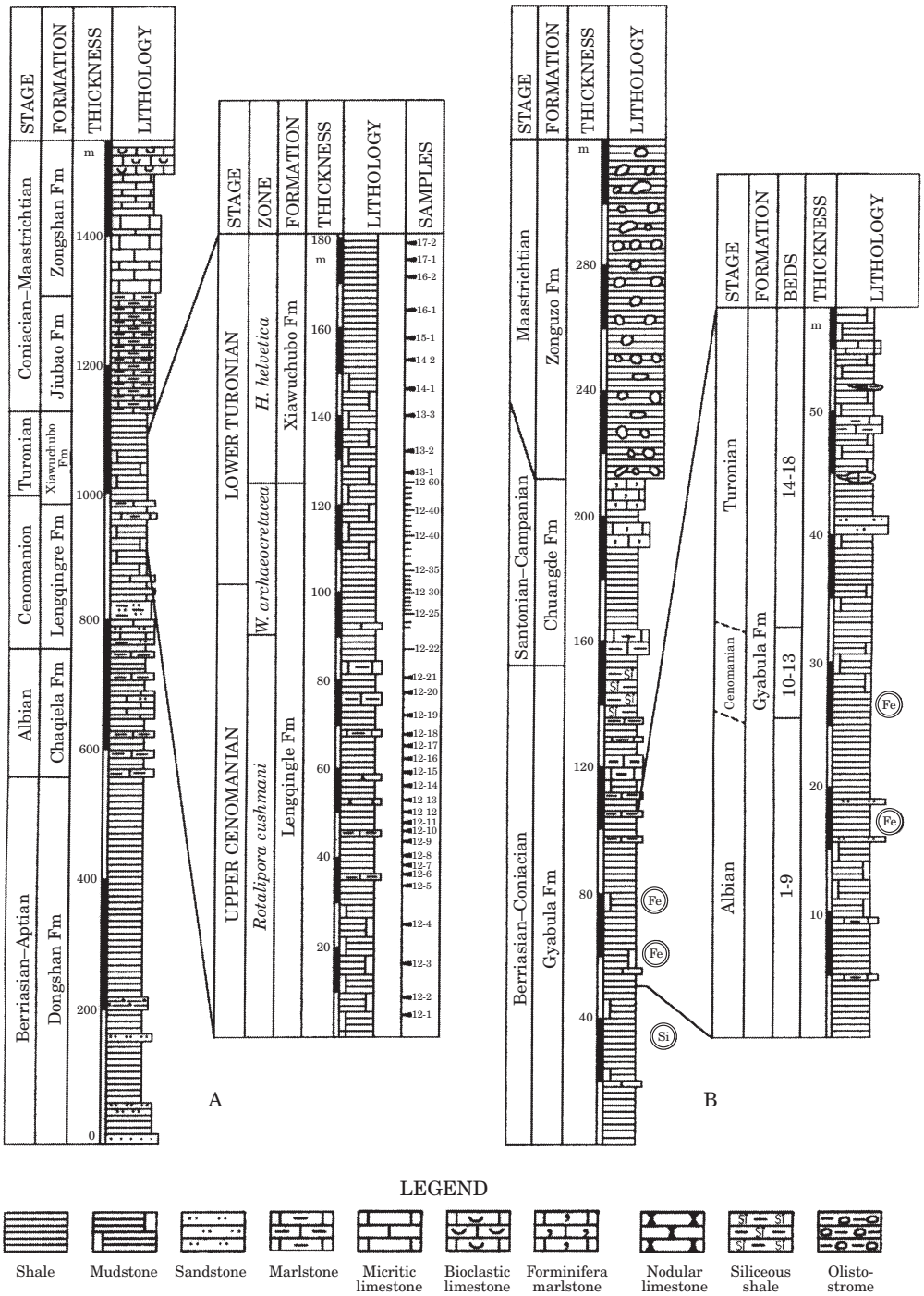

Figure 2. Lithostratigraphy of the Cretaceous strata and data for the CTB in southern Tibet. A, Zongshan; B, Gyabula.

consists of violet-red marlstones and mudstones. Two foraminiferal zonal-marker species, *Dicarinella asymetrica* and *Globotruncana ventricosa*, have been recovered from the red marls, indicating their Santonian–early Campanian age (Robaszynski & Caron, 1995). The overlying Zongzhuo Formation is of late Campanian–Maastrichtian age and predominantly composed of dark grey to black shales enclosing various olistoliths of sandstone, limestone, and siliceous rocks, corresponding to the 'Beijia Olistostrome' (Liu & Einsele, 1994).

At the Gyabula locality, east of Gyangze (Figure 1), radiolarians and planktonic foraminifera both define the base and the top of the Cenomanian. Beds 8–9

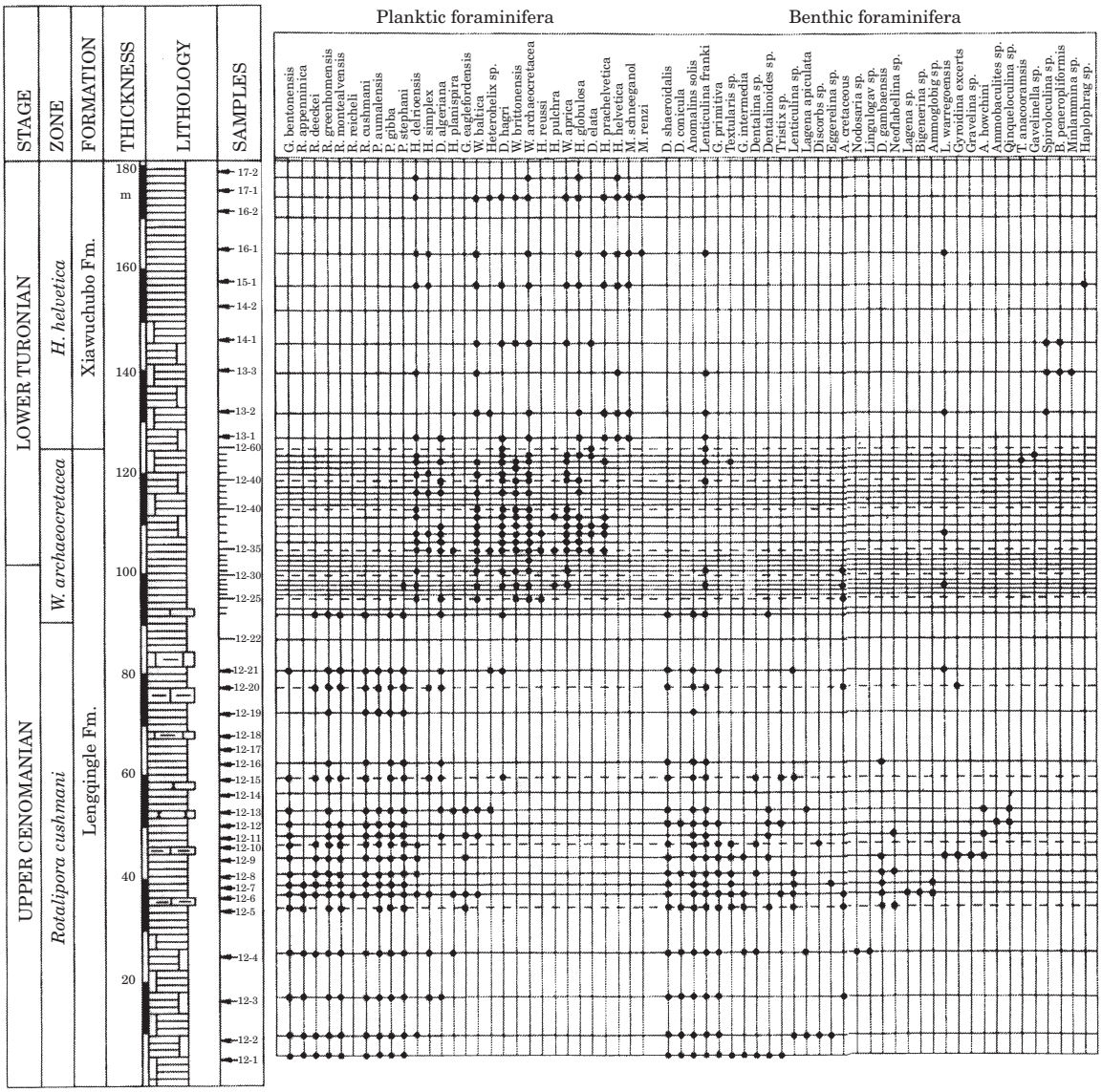

Figure 3. Biostratigraphic ranges of planktonic and benthic foraminifera at the Zongshan locality.

(Figure 2B) yield radiolarian genera including *Artocapsa* sp., *Cyrtocapsa campi*, *Praestylosphaera hastata*, and *Pseudodictyomitra pseudomacrocephala*, indicating an Albian age. Bed 10 yields *Dictyomitra* sp. and *Stichocapsa* sp., indicating a Cenomanian age. The Albian/Cenomanian boundary is, therefore, placed between beds 9 and 10. A younger radiolarian assemblage is found in bed 14. It includes *Gavidiscus* sp., *Grongylothorax siphonofer*, *Obesacapsula* sp., *Pseudotheocampe ascalia*, and *Tricolocapsa rusti*. At this locality, it remains difficult to locate precisely the CTB owing to the absence of fossils. However, it was tentatively placed between beds 13 and 14 because older foraminifera such as *Rotalipora* and *Hedbergella* appear in bed 13, while beds 15–16 contain *Whiteinella archaeocretacea* (Figure 2).

3. Lithostratigraphy and depositional setting

At the Zongshan locality (Gamba area), the mid-Cretaceous strata are represented by the Chaqiela, Lengqingre, and Xiawuchubo formations. The upper part of the Chaqiela Formation (beds 16–27) consists

of muddy, calcareous, glauconite-bearing, fine-grained sandstones. Quartz grains, which are the major component, are mostly angular and frequently shard-shaped, indicating minimal reworking and rapid deposition. Feldspars are a minor component, while mica, zircon, rutile and foraminiferal tests are rare. The sandstones are interbedded with greenish and dark grey shales and thin beds of sandy and silty foraminiferal biomicrites. The presence of glauconitic sandstones suggests deposition on an outer shelf. The overlying Lengqingre Formation (beds 28–42) is composed of black shales and calcareous shales intercalated with nodular to thin-bedded limestones. The limestones are predominately argillaceous biomicrites and biomicrosparites with scattered foraminifera, calcispheres, ostracoda, sponge spicules (?), and nannofossils. In some limestone beds laminae of quartz silt are present. Some of the limestones are bioturbated. Carbonate content decreases upwards within this formation. The depositional environment was most probably upper continental slope, as indicated by the occurrence of silt-sized peloid packstones, and by the hemipelagic character of the limestone deposits which lack a shelf-type fauna.

The upper Xiawuchubo Formation (beds 43–50) is largely composed of yellow and blue shales intercalated with thin-bedded limestones and marls. Carbonate content increases upwards in the formation. Inoceramid bivalves are abundant along with variable numbers of thick-walled molluscs, echinoids, ostracoda, thin-walled pelagic molluscs and phosphatic fish debris. Quartz silt is rare and dispersed within the carbonate. The sediment composition indicates that deposition occurred on the deep outer shelf or perhaps on the upper continental slope, with the environment shallowing upwards.

The Upper Cenomanian–Lower Turonian black shales at the Zongshan locality are predominately laminated and occasionally contain trace fossils. The calcium carbonate content in the shales varies from 18 to 37%. The total organic carbon (TOC) ranges from 0.5 to 1.7%. In contrast to the black shale facies, the interbedded lighter coloured mudstones and marlstones are irregularly laminated to massive and weakly bioturbated. Calcium carbonate content ranges from 14 to 70%, and TOC from 0.4 to 0.5%. X-ray diffraction shows that the dominant clay mineral is illite (42–71%), with chlorite (21–24 %) and kaolinite (12–15%) in subordinate amounts.

In the Gyangze area, the middle Cretaceous strata represented by the upper part of the Gyabula Formation are composed of black shales intercalated with siliceous shales (Wu *et al.*, 1977; Xu *et al.*, 1990; Li *et al.*, 1999; Wang *et al.*, 2000). Pyrite concretions, up to 80 cm in diameter, are common. The black shales have relatively high TOC (*c.* 1.2%) and low calcium carbonate (*c.* 17%). The bottom feeding trace fossil *Chondrites* is abundant and suggests poorly oxygenated bottom-water conditions (Savrda & Bottjer, 1986).

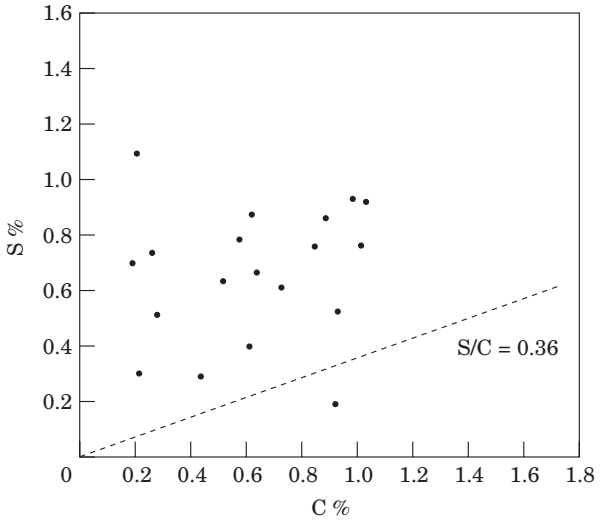

Figure 4. Sulfur(S)/Carbon(C) ratio at the CTB, Gyabula, indicating a dysoxic depositional environment.

The TOC values of the CTB black shales in southern Tibet are generally lower than in western Tethys. In Europe the TOC at the CTB is typically higher than 10%, with a range of 1.3–31.2% (Farrimond *et al.*, 1990). It is also higher in the Santos Basin of Brazil (Trindade *et al.*, 1996). The low TOC values in southern Tibet could be the result of oxidation and weathering of strata during the Cenozoic when the Qinghai-Tibet Plateau was tectonically deformed (Hauck *et al.*, 1998). Alternatively, southern Tibet could have had a lower supply, or decreased preservation, of organic carbon during the mid Cretaceous.

4. Sulfur content as evidence of a euxinic environment

To investigate the depositional environment further, the sulfur content of the middle Cretaceous deposits of both the Gamba and Gyangze areas was studied. Bulk rock sulfur/carbon (S/C) ratios greater than 0.36 have been used to infer euxinic conditions (Berner & Raiswell, 1984; Raiswell & Berner, 1985; Minster *et al.*, 1992; Morse & Berner, 1995). The S/C ratio in rocks at Gyabula is greater than 0.36 (Figure 4), suggesting that the depositional environment was anoxic. In the Gamba area at Zongshan, the S/C ratios

are very low, *c.* 0.05, mainly owing to very high Fe^{3+}/Fe^{2+} ratios and low sulfur content. The Fe^{3+}/Fe^{2+} ratio at Gyabula is seven times lower than at Zongshan, and the sulfur content in Gyangze is 32 times higher than at Gamba, where it is only 0.02%.

In middle Cretaceous black shales at Zongshan the iron is mainly concentrated in siderites, glauconites and pyrites. The increased content of Fe may have been the result of detrital input from a continental source, or a diagenetic effect owing to the oxidation of organic matter and the development of an anoxic, early diagenetic environment condusive to iron sulphide precipitation.

Degree of pyritization (DOP, the ratio of Fe in sulphide minerals to total reactive Fe) has been used as an indicator of early diagenetic reducing environments, and has been indirectly applied as an indicator of euxinic conditions (Raiswell & Berner, 1985). Raiswell *et al.* (1988) suggested that a DOP of <0.45 indicates oxic bottom waters; of >0.45–<0.75 indicates dysoxic bottom waters; and of >0.75 indicates anoxic bottom-water conditions. Most shales at Gyabula have DOP values between 0.60 and 0.75 (average 0.68), which indicates a 'dysoxic' depositional environment. In contrast, DOP values for Gamba are <0.36, indicating oxic bottom conditions.

5. Carbon isotopes

Diagenesis can adversely affect carbon isotope composition. At Zongshan, preservation of calcareous shells and formation of clotted micrite fabric suggest that Cretaceous limestones experienced only low diagenetic transformation. They are, therefore, suitable for whole-rock carbon-isotope analysis. The $\delta^{13}C$ excursion across the CTB (Figure 5) varies from -0.4 to $+2.7‰$. The positive $\delta^{13}C$ excursion corresponds well with CTB localities in other parts of the world (e.g., Arthur *et al.*, 1987; Arthur & Sageman, 1994). The isotope curve shows three peaks across the CTB, also recognized in the US Western Interior localities of the Greenhorn Formation (Pratt, 1985) and in England (Gale *et al.*, 1993).

6. Micropalaeontological trends

The micropalaeontology of middle Cretaceous deposits in Gamba has been studied by several authors (Wan, 1985; Xu & Mao, 1992; Wan & Yin, 1996; Wan *et al.*, 1997). In this paper changes in the patterns of the microfossil assemblages across the CTB are documented.

Foraminifera decrease in abundance gradually from the bottom to the top of the Upper Cenomanian *Rotalipora cushmani* Zone, and then rapidly decrease in the *Whiteinella archaeocretacea* Zone, to the point at which they nearly disappear before gradually increasing again into the Lower Turonian *Helvetoglobotruncana helvetica* Zone. The diversity of planktic foraminifera declines into the *Whiteinella archaeocretacea* Zone and increases in the overlying *Helvetoglobotruncana helvetica* Zone (Figure 6). The diversity of benthic foraminifera shows a similar trend. They are absent through most of the CTB interval and recover only slightly at the base of the *Helvetoglobotruncana helvetica* Zone (Figure 6).

The ratio of keeled/non-keeled planktic foraminifera can be used as an indicator of open marine environments and epipelagic conditions (Leckie, 1987). At the Zongshan locality, the ratio decreases dramatically at the base of the *Whiteinella archaeocretacea* Zone, reaches a minimum at the CTB, and then recovers in the lower part of the Turonian section (Figure 6).

The trend in abundance and diversity of foraminifera across the CTB in the Gamba area differs from, for example, the trend in the US Western Interior where foraminiferal abundance is high at the top of the *Rotalipora cushmani* Zone and decreases into the *Whiteinella archaeocretacea* Zone, and then increases in the Lower Turonian (Scott *et al.*, 1998). Foraminiferal trends in the Western Interior during the Middle Cenomanian–Middle Turonian were affected by transgressive-regressive cycles. The diversity of foraminifera declines slightly across the CTB interval and keeled planktic taxa also decrease in abundance through this interval (Scott *et al.*, 1998), as similarly observed in Gamba.

Foraminiferal data from the CTB in southern Tibet clearly record a global deterioration in marine environmental conditions. Extinction rates for planktic foraminiferal species are 50–70%, and up to 90% for the benthics at the CTB in the Gamba section. The extinction of the planktonic foraminifera is much higher than the *c.* 20% global average estimated for the Bonarelli Event by M. Leckie (pers. comm., 2000). Kaiho (1994) related this event in the Pacific to a decreased content of dissolved oxygen in intermediate waters. In the Pacific the extinction rates of planktic foraminifera across the CTB was 28% (Sliter, 1989), whereas the global extinction rates were calculated to be around 41% (Caron, 1985). The extinction rates of benthic foraminifera increase from open oceanic settings, e.g., 37% in Japan (Kaiho & Hasegawa, 1994), to 53% recorded in epicontinental seas, such as in Poland (Peryt & Wyrwicka, 1991), 58% in England (Jarvis *et al.*, 1988), and 69% in the US Western Interior seaway (Eicher & Worstell,

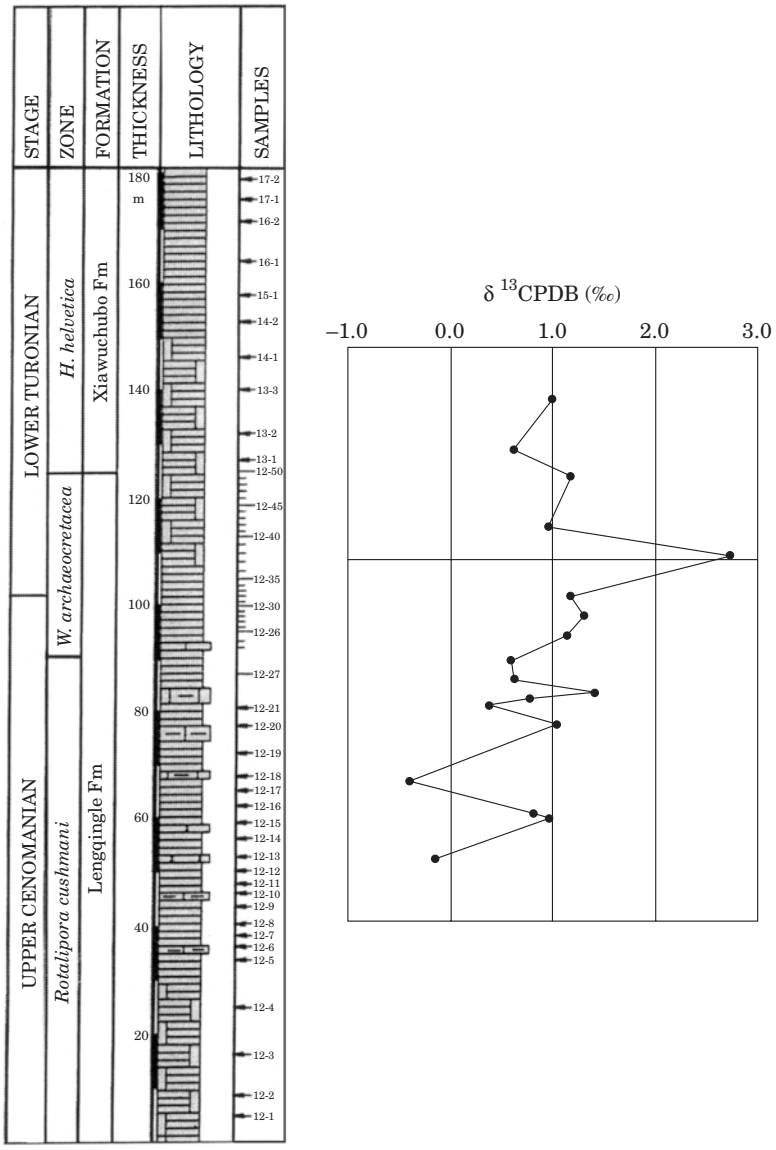

Figure 5. $\delta^{13}C$ data for carbonate in uppermost Cenomanian–lowermost Turonian strata at Zongshan showing a positive excursion of 2‰.

1970). It is apparent that the extinction of foraminifera was highest in southern Tibet. Why the extinction was so high while the content of organic carbon was lower than in many areas of Tethys remains unanswered and will be the subject of future studies.

7. Conclusion

The CTB black shale sequence exposed in southern Tibet records a global oceanic anoxic event (OAE). The shales are enriched in organic carbon, with TOC concentrations varying from 0.5 to 1.7%. Analyses of S/C and DOP indicate that the slope depositional environment in the Gyangze area was oxygen-depleted (dysoxic) and H_2S-rich. By contrast, bottom conditions on the shelf were oxic in the Gamba area. Whole rock $\delta^{13}C$ analyses across the CTB document the presence of a positive excursion of *c.* 2‰, as similarly observed in the western Tethys. Microfossil studies in southern Tibet document increasing extinction rates of planktic and benthic foraminifera across the CTB, when they reached a maximum. The extinction ratio of planktic foraminifera across the CTB was 50–70%, while for the benthic foraminifera was up to 90%. The presence of a CTB OAE in Tibet indicates that a layer of poorly oxygenated bottom and intermediate waters developed within the Tethys as a result of fundamental changes in Late Cretaceous

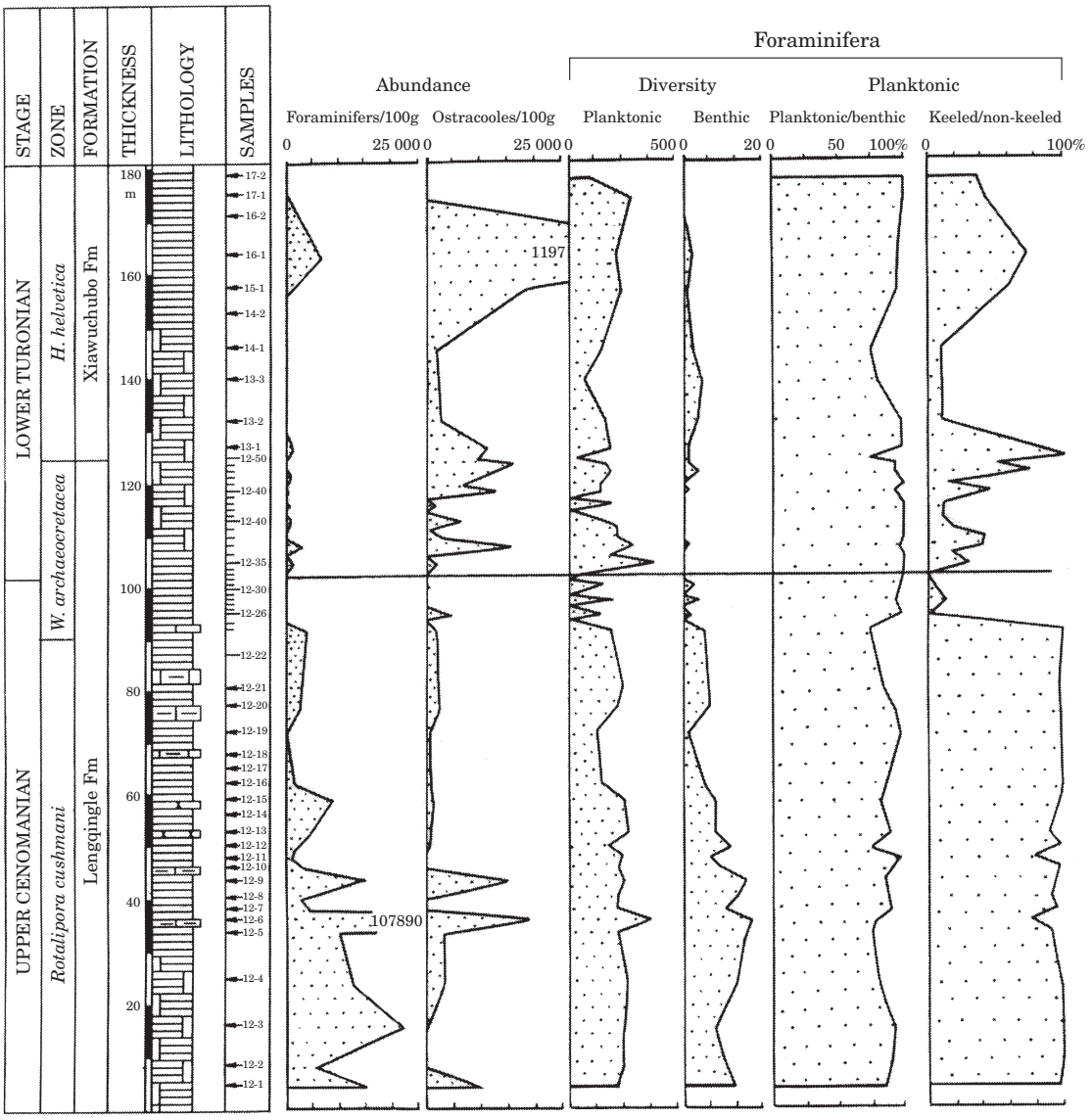

Figure 6. Stratigraphic plot of changes in abundance of ostracods, in abundance and diversity of foraminifera, and in the ratio of planktonic to benthic and keeled to non-keeled foraminifera at Zongshan.

palaeoceanographic patterns. These changes were most probably associated with increased dispersal of the southern continent, as the Indian plate moved northwards. The shelf areas remained in oxic waters as a result of wind-induced mixing of surface water.

Acknowledgements

We acknowledge helpful comments on the manuscript by Drs R. W. Scott, T. J. Bralower, M. Leckie, and K. Kaiho. Prof. D. J. Batten and two anonymous reviewers are thanked for their reviews which improved the paper. We also thank Drs Zeng Yunfu, Li Xianghui, and Li Hongsheng for their support and encouragement. The study has been supported by the National Foundation for Outstanding Young Scientists in China (No. 49625203) and the China National Natural Science Foundation (No. 0487005).

References

Arthur, M. A. & Sageman, B. B. 1994. Marine black shales: depositional mechanisms and environments of ancient deposits. *Annual Review of Earth and Planetary Sciences* **22**, 499–551.

Arthur, M. A., Schlanger, S. O. & Jenkyns, H. C. 1987. The Cenomanian–Turonian oceanic anoxic event; II. Palaeoceanographic controls on organic-matter production and preservation. In *Marine petroleum source rocks* (eds Brooks, J. & Fleet, A. J.), *Geological Society, London, Special Publication* **26**, 401–420.

Berner, R. A. & Raiswell, R. 1984. C/S method for distinguishing freshwater from marine sedimentary rocks. *Geology* **12**, 365–368.

Bralower, T. J. 1988. Cenomanian–Turonian oceanic anoxic event; local perturbations on a global theme. *American Association of Petroleum Geologists, Bulletin* **72**, 165–166.

Caron, M. 1985. Cretaceous planktonic foraminifera. In *Plankton stratigraphy* (eds Bolli, H. M., Saunders, J. B. & Perch-Nielsen, K.), pp. 17–86 (Cambridge University Press, Cambridge).

Crumière, J. P. 1988. Paleoceanographic controls of a source rock (Thomel level) deposition; anoxic event around the Cenomanian–Turonian boundary in southeastern France. In *Mediterranean basins conference and exhibition. American Association of Petroleum Geologists, Bulletin* **72**, 996.

Eicher, D. L. & Worstell, P. 1970. Cenomanian and Turonian foraminifera from the Great Plains, United States. *Micropaleontology* **16**, 269–324.

Farrimond, P., Eglinton, G. & Brassell, S. C. 1990. The Cenomanian–Turonian anoxic event in Europe: an organic geochemical study. *Marine and Petroleum Geology* **7**, 75–89.

Gale, A. S., Jenkyns, H. C., Kennedy, W. J. & Corfield, R. M. 1993. Chemostratigraphy versus biostratigraphy: data from around the Cenomanian–Turonian boundary. *Journal of Geological Society, London* **150**, 29–32.

Govindan, A. & Ramesh, P. 1995. Cretaceous anoxic events and their role in generation and accumulation of hydrocarbons in Cauvery Basin, India. *Indian Journal of Petroleum Geology* **4**, 1–15.

Hasegawa, T. & Saito, T. 1993. Global synchroneity of a positive carbon isotope excursion at the Cenomanian/Turonian boundary: validation by calcareous microfossil biostratigraphy of the Yeza Group, Hokkaido, Japan. *The Island Arc* **2**, 181–191.

Hauck, M. L., Nelson, K. D., Brown, L. D., Zhao, W. J. & Ross, A. R. 1998. Crustal structure of the Himalayan orogen at 90 degrees east longitude from Project INDEPTH deep reflection profiles. *Tectonics* **17**, 481–500.

Herbin, J. P., Muller, C., de Graciansky, P. C., Jacquin, T., Magniez, J. F. & Unternehr, P. 1987. Cretaceous anoxic events in the South Atlantic. *Revista Brasileira de Geociencias* **17**, 92–99.

Hilbrecht, H. & Dahmer, D. 1994. Sediment dynamics during the Cenomanian–Turonian (Cretaceous) oceanic anoxic event in northwestern Germany. *Facies* **30**, 63–84.

Jarvis, I., Carson, G., Hart, M., Leary, P. & Tocher, B. A. 1988. The Cenomanian–Turonian (Late Cretaceous) anoxic event in SW-England; evidence from Hooken Cliffs near Beer, SE Devon. *Newsletters on Stratigraphy* **18**, 147–164.

Jenkyns, H. C. 1980. Cretaceous anoxic events: from continents to oceans. *Journal of the Geological Society, London* **137**, 171–188.

Kaiho, K. 1994. Planktonic and benthic foraminiferal extinction events during the last 100 m.y. *Palaeogeography, Palaeoclimatology, Palaeoecology* **111**, 45–71.

Kaiho, K. & Hasegawa, T. 1994. End-Cenomanian benthic foraminiferal extinctions and oceanic dysoxic events in the northwestern Pacific Ocean. *Palaeogeography, Palaeoclimatology, Palaeoecology* **111**, 29–43.

Leary, P. N., Carson, G. A., Cooper, M. K. E., Hart, M. B., Horne, D., Jarvis, I., Rosenfeld, A. & Tocher, B. A. 1989. The biotic response to the late Cenomanian oceanic anoxic event; integrated evidence from Dover, SE England. *Journal of the Geological Society, London* **146**, 311–317.

Leckie, R. M. 1987. Paleoecology of mid-Cretaceous planktonic foraminifera: a comparison of open ocean and epicontinental sea assemblages. *Micropaleontology* **33**, 164–176.

Li, X. H., Wang, C. S., Wan, X. Q. & Tao, R. 1999. Verification of stratigraphic sequence and classification for the Chuangde cross-locality of Gyangze, southern Tibet. *Journal of Stratigraphy* **23**, 303–309. [In Chinese, English abstract]

Liu, G. & Einsele, G. 1994. Sedimentary history of the Tethyan basin in the Tibetan Himalayas. *Geologische Rundschau* **83**, 32–61.

Mello, M. R., Koutsoukos, E. A. M., Hart, M. B., Brassell, S. C. & Maxwell, J. R. 1989. Late Cretaceous anoxic events in the Brazilian continental margin. *Organic Geochemistry* **14**, 529–542.

Minster, T., Nathan, Y. & Raveh, A. 1992. Carbon and sulfur relationships in marine Senonian organic-rich, iron-poor sediments from Israel – a case study. *Chemical Geology* **97**, 145–161.

Morse, W. J. & Berner, A. R. 1995. What determines sedimentary C/S ratios. *Geochimica et Cosmochimica Acta* **59**, 1073–1077.

Mu, A. Z., Wen, S. X., Wang, Y. G., Zhang, B. G. & Yin, J. X. 1973. Stratigraphy of the Mount Jolmoo Lungma region in south Tibet. *Science in China* **16**, 96–111. [In Chinese, English abstract]

Patzelt, A., Li, H., Wang, J. & Appel, E. 1996. Palaeomagnetism of Cretaceous to Tertiary sediments from southern Tibet: evidence for the extent of the northern margin of India prior to the collision with Eurasia. *Tectonophysics* **259**, 259–284.

Paul, C. R. C., Mitchell, S., Lamolda, M. & Gorostidi, A. 1994. The Cenomanian–Turonian boundary event in north Spain. *Geological Magazine* **131**, 801–817.

Peryt, D. & Wyrwicka, K. 1991. The Cenomanian–Turonian oceanic anoxic event in SE Poland. *Cretaceous Research* **12**, 65–80.

Pratt, L. M. 1985. Isotopic studies of organic matter and carbonate in rocks of the Greenhorn marine cycle. In *Fine-grained deposits and biofacies of the Western Interior Seaway: evidence of cyclic sedimentary processes* (eds Pratt, L. M., Kauffman, E. G. & Zelt, F. B.), *Field Trip Guidebook No. 4, Society of Economic Paleontologists and Mineralogists, Tulsa*, pp. 38–48.

Raiswell, R. & Berner, R. A. 1985. Pyrite formation in euxinic and semi-euxinic sediments. *American Journal of Science* **285**, 710–724.

Raiswell, R., Buckley, F., Berner, R. A. & Anderson, T. F. 1988. Degree of pyritization of iron as a palaeoenvironmental indicator of bottom-water oxygenation. *Journal of Sedimentary Petrology* **58**, 812–819.

Reyment, R. A. & Bengtson, P. (compilers) 1986. *Events of the mid-Cretaceous physics and chemistry of the Earth,* 213 pp. (Pergamon Press, Oxford).

Robaszynski, F. & Caron, M. 1995. Foraminifères planctoniques du Crétacé: commentaire de la zonation Europe-Méditerranée. *Bulletin de la Société Géologique de France* **166**, 681–692.

Savrda, C. E. & Bottjer, D. J. 1986. Trace-fossil model for reconstruction of paleo-oxygenation of bottom waters. *Geology* **14**, 3–6.

Schlanger, S. O. & Jenkyns, H. C. 1976. Cretaceous oceanic anoxic events: cause and consequence. *Geologie en Mijnbouw* **55**, 179–184.

Schlanger, S. O., Arthur, M. A., Jenkyns, H. C. & Scholle, P. A., 1987. The Cenomanian–Turonian oceanic anoxic event, I. Stratigraphy and distribution of organic carbon-rich beds and the marine $\delta^{13}C$ excursion. In *Marine petroleum source rocks* (eds Brooks, J. & Fleet, A. J.), *Geological Society, London, Special Publication* **26**, 371–399.

Scott, R. W., Franks, P. C., Evetts, M. J., Bergen, J. A. & Stein, J. A. 1998. Timing of mid-Cretaceous relative sea level changes in the Western Interior: Amoco No.1 Bounds Core. In *Stratigraphy and paleoenvironments of the Cretaceous Western Interior Seaway, USA* (eds Dean, W. A. & Arthur, M. A.), *SEPM* (*Society for Sedimentary Geology*), *Concepts in Sedimentology and Paleontology* **6**, 11–34.

Sliter, W. V. 1989. Biostratigraphic zonation for Cretaceous planktonic foraminifers examined in thin section. *Journal of Foraminiferal Research* **19**, 1–9.

Trindade, L. A. F., Porsche, E., Penteado, H. L. B., Botelho, N. J., Araujo, C. V., Viviers, M. C. & Oliveira, L. C. V. 1996. Geochemical and biostratigraphic characterization of an Upper Cretaceous organic-rich condensed section in the Santos Basin, Brazil. In *American Association of Petroleum Geologists, 1996 annual convention, Tulsa, Abstracts,* p. 567.

Wan, X. Q. 1985. Cretaceous strata and foraminifera of Gamba region, Xizang (Tibet). *Contribution to the Geology of the Qinghai-Xizang* (*Tibet*) *Plateau* **16**, 203–228. [In Chinese, English abstract]

Wan, X. Q., Lamolda, M. A. & Wang, C. S. 1997. Upper Cenomanian–Lower Turonian foraminiferal assemblages from

southern Tibet: the responses of the biota to oceanic environmental change. *Journal of the Geological Society of the Philippines* **52**, 183–197.
Wan, X. Q. & Yin, J. R. 1996. Mid-Cretaceous microfossil assemblages and palaeoceanographic event in Gamba, Tibet. *Acta Micropalaeontologica Sinica* **13**, 43–56. [In Chinese, English abstract]
Wang, C. S., Li, X. H., Wan, X. Q. & Tao, R. 2000. Reform of the Cretaceous in Gyangze, South Tibet. *Acta Geologica Sinica* **74**, 97–107. [In Chinese, English abstract]
Wen, S. X. 1974. The stratigraphy of the Mount Jomulongma region: Cretaceous and Tertiary. In *Report on scientific expedition in the Mount Jomulongma region, 1966–1968: Geology*. pp. 148–214 (Science Press, Beijing). [In Chinese, English abstract]
Willems, H. & Zhang, B. 1993. Cretaceous and Lower Tertiary sediments of the Tibetan Tethys Himalaya in the area of Gamba (South Tibet, PR China). In *Geoscientific investigation in the Tethyan Himalayas* (ed. Willems, H.), *Berichte, Fachbereich Geowissenschaften, Universität Bremen* **38**, 3–28.
Wu, H. R. 1987. The strata of Late Cretaceous and Early Tertiary (?) in Gyangze area, South Tibet. *Journal of Stratigraphy* **11**, 147–150. [In Chinese, English abstract]
Wu, H. R., Wang, D. & Wang, L. 1977. The Cretaceous of Lazhi-Gyangze district, southern Xizang. *Acta Geologica Sinica* **3**, 250–262. [In Chinese, English abstract]
Xu, Y. L. & Mao, S. Z. 1992. Cretaceous–early Tertiary calcareous nannofossil from southern Xizang (Tibet) and their sedimentary environment. *Acta Micropalaeontologica Sinica* **9**, 331–347. [In Chinese, English abstract]
Xu, Y. L., Wan, X. Q., Gou, Z. H. & Zhang, Q. H. 1990. *Biostratigraphy of Xizang, Tibet, in the Jurassic, Cretaceous and Tertiary periods*, 147 pp. (China University of Geosciences Press, Wuhan). [In Chinese, English abstract]
Yu, G. M. & Wang, C. S. 1990. *Sedimentary geology of the Xizang, Tibet, Tethys.* vii+185 pp., 23 pls (Geological Publishing House, Beijing). [In Chinese, English abstract]

Appendix

Alphabetical list of taxa mentioned in text with authorities and dates.

Foraminifera
Ammobaculites sp.
Ammodiscus cretaceus Reuss, 1845
Ammoglobigerina sp.
Anomalina solis Nauss, 1947
Astacolus howchini Ludbrook, 1966
Bigenerina sp.
Biplanata peneropliformis Hamaoui & Saint-Marc, 1970
Dentalina sp.
Dentalinoides sp.
Dicarinella algeriana Caron, 1966
Dicarinella asymetrica Sigal, 1952
Dicarinella elata Lamolda, 1978
Dicarinella hagni Scheibnerova, 1962
Discorbis sp.
Dorothia conicula Belford, 1960
Dorothia gambaensis Wan, 1985
Dorothia shaeroidalis Wan, 1985
Eggerellina sp.
Gavelinella intermedia Berthelin, 1880
Gavelinella sp.
Globigerinelloides bentonensis Morrow, 1934
Globigerinelloides eaglefordensis Morman, 1961
Globotruncana ventricosa White, 1928
Gravelina sp.
Gyroidina excerta Belford, 1960
Gyrodinoides primitiva Hofker, 1957
Haplophragmoides sp.
Hedbergella delrioensis Carsey, 1926
Hedbergella planispira Tappan, 1940
Hedbergella simplex Morrow, 1934
Hedbergella trocoidea Gandolfi, 1942
Helvetoglobotruncana helvetica Bolli, 1945
Helvetoglobotruncana praehelvetica Trujillo, 1960
Heterohelix globulosa Ehrenberg, 1840
Heterohelix pulchra Brotzen, 1936
Heterohelix reussi Cushman, 1938
Heterohelix sp.
Lagena apiculata Reuss, 1851
Lagena sp.
Lenticulina franki Marie, 1941
Lenticulina warregoensis Crespin, 1944
Lenticulina sp.
Lingulogavelinella sp.
Marginotruncana renzi Gandolfi, 1942
Marginotruncana schneegansi Sigal, 1952
Miniammina sp.
Neoflabellina sp.
Nodosaria sp.
Praeglobotruncana aumalensis Sigal, 1925
Praeglobotruncana gibba Klaus, 1960
Praeglobotruncana stephani Gandolfi, 1942
Quinqueloculina sp.
Rotalipora appenninica Renz, 1936
Rotalipora cushmani Morrow, 1934
Rotalipora deeckei Franke, 1925
Rotalipora greenhornensis Morrow, 1934
Rotalipora montsalvensis Mornod, 1949
Rotalipora reicheli Mornod, 1949
Spiroloculina sp.
Textularia anacooraensis Crespin, 1953
Textularia sp.
Tristix sp.
Whiteinella aprica Loeblich & Tappan, 1961
Whiteinella archaeocretacea Pessagno, 1967
Whiteinella baltica Douglas & Rankin, 1969
Whiteinella brittonensis Loeblich & Tapan, 1961

Radiolaria
Artocapsa sp.
Cyrtocapsa campi Clark & Campbell, 1945
Dictyomitra sp.
Eucyriticium sp.
Gavidiscus sp.
Grongylothorax siphonofer Dumitrica, 1970
Hemicryptocapsa sp.
Obesacapsula sp.
Praestylosphaera hastata (Campbell & Clark, 1944)
Pseudoaulacophacus floresensis Pessagno, 1963
Pseudodictyomitra pseudomacrocephala Squinabal, 1903
Pseudotheocampe ascalia, Abschnitta & Empson-Morin, 1981
Stichocapsa sp.
Theocampe tina Foreman, 1971
Tricolocapsa rusti Tan, 1926